

A Cat-State Benchmark on a Seven Bit Quantum Computer

E. Knill¹(CIC-3), R. Laflamme¹(T-6)
R. Martinez¹ (CST-4), C.-H. Tseng²

¹*Los Alamos National Laboratory*

²*Dept. of Nuclear Engineering, MIT, Cambridge, MA 02139*

We propose and experimentally realize an algorithmic benchmark that demonstrates coherent control with a sequence of quantum operations that first generates and then decodes the cat state $(|000\dots\rangle + |111\dots\rangle)/\sqrt{2}$ to the standard initial state $|000\dots\rangle$. This is the first high fidelity experimental quantum algorithm on the currently largest physical quantum register, which has seven quantum bits (qubits) provided by the nuclei of crotonic acid. The experiment has the additional benefit of verifying a seven coherence in a generic system of coupled spins. Our implementation combines numerous nuclear magnetic resonance (NMR) techniques in one experiment and introduces practical methods for translating quantum networks to control operations. The experimental procedure can be used as a reliable and efficient method for creating a standard pseudo-pure state, the first step for implementing traditional quantum algorithms in liquid state NMR. The benchmark and the techniques can be adapted for use on other proposed quantum devices.

Quantum information processing (QIP) offers significant advantages over classical information processing, both for efficient algorithms [30,29] and for secure communication [33,3]. As a result it is important to establish that sufficient and scalable control of a large number of qubits can be achieved in practice. There are a rapidly growing number of proposed device technologies [9,22,4,27,10,14,25,17] for QIP, and to compare them it is necessary to establish benchmark experiments that are independent of the underlying physical system. A good benchmark for QIP should demonstrate the ability to reliably and coherently control a reasonable number of qubits. This requires that elementary operations can be implemented with small error regardless of the state of the qubits, as sufficiently small error is one of the most important prerequisites for robust QIP [28,1,18,20]. The cat-state benchmark proposed here is perhaps the simplest demonstration of control which can be implemented for any number of qubits and involves coherence in a non-trivial way.

To explain and realize the cat-state benchmark we use the example of NMR based QIP. At least two proposals for quantum devices are based on using nuclear spins controlled by radio frequency (RF) fields: The first involves the use of molecules [10,14] forming an ensemble of quantum registers and the second uses nuclei embedded in a semiconductor [25,17]. Of these proposals, the first is

presently accessible to experimental investigation by the use of off-the-shelf equipment for liquid state NMR. By means of the technique of preparing pseudo-pure states, it is possible to benchmark quantum algorithms involving up to about ten qubits to determine how well coherence is preserved and to measure how reliable the available control methods are. There have been numerous experiments implementing various quantum algorithms on up to five qubits [15,8,16,6,7,21,11,24,23] using NMR. The experiment reported here coherently implements a quantum algorithm on seven qubits with a verifiable fidelity. It also introduces a reliable method for preparing pseudo-pure states and for verifying maximal coherences in generic spin systems.

NMR QIP uses spin $\frac{1}{2}$ nuclei as qubits. Examples are protons and carbon 13 bound in a molecule. QIP requires the ability to couple different qubits. In molecules in a liquid at high magnetic field, scalar couplings can be used for this purpose and controlled with refocusing methods [10,14]. Thus, each molecule can be considered as a quantum register consisting of (some of) its spin $\frac{1}{2}$ nuclei. The initial state is prepared by allowing enough time for thermal relaxation and readout is performed by an ensemble measurement using standard NMR methods. We use deviation density matrices [31] for describing the state of the nuclei. To simplify the discussion, we use a three qubit example of the cat-state benchmark. The thermal equilibrium state of a molecule with one proton and two carbon 13 nuclei at high field in a liquid is given by $\sigma_z^{(H)} + .25\sigma_z^{(C_1)} + .25\sigma_z^{(C_2)}$ with high accuracy, up to an overall scale factor and a multiple of the identity. The standard Pauli matrices are used as an operator basis, and superscripts on operators refer to the particle the operator acts on. The cat-state benchmark for this system begins by eliminating signal from the carbons to obtain the initial state $\sigma_z^{(H)}$. Next a sequence of quantum gates [2] is used to achieve the state $\sigma_y^{(H)}\sigma_y^{(C_1)}\sigma_x^{(C_2)}$ (Fig.1). This state is a sum of several coherences [13]. In particular, it contains the three coherence $|000\rangle\langle 111| + |111\rangle\langle 000|$, which is the deviation of the operator for the cat state $(|000\rangle + |111\rangle)/\sqrt{2}$. If each qubit is rotated by a phase ϕ around the z -axis, the three coherence rotates by 3ϕ , while all other components of this (or any other) state will rotate by 0 , ϕ or 2ϕ . This feature can be used to label the three coherence and eliminate all other components of the state, for example by using a magnetic field gradient [13]. An efficient alternative using z -pulses or phase cycling is given below. The three coherence can be decoded to the state $\sigma_x^{(H)}|00\rangle\langle 00|$

(Fig.1). This is then observed after inverting the labeling gradient at three times the original strength. In a fully resolved reference spectrum obtained by applying a 90deg rotation to the proton in the initial state, the proton shows four peaks, one for each of the states $|00\rangle\langle 00|$, $|01\rangle\langle 01|$, $|10\rangle\langle 10|$ and $|11\rangle\langle 11|$ of the carbons. After decoding the cat state, only a single peak should be left in the spectrum. The ratio F of the intensity of this peak to the intensity of the corresponding peak in the reference spectrum is unity if everything works perfectly. F is reduced by errors in the preparation and decoding steps. Under the assumption that error in the phase labeling method is negligible, it can be shown that F is a lower bound on the average of the fidelities [26] with which the decoding procedure maps the states $|000\rangle \pm |111\rangle$ to the states $(|0\rangle \pm |1\rangle)|00\rangle$.

The three qubit cat-state benchmark can be generalized to any number n of qubits by repeating the steps of the cascade in the networks shown in Fig.1. We implemented the seven qubit version using fully labeled transcrotonic acid (Fig.2). The qubits are given by the spin $\frac{1}{2}$ component of the methyl group, the two protons adjacent to the double bond and the four carbon 13 nuclei. A fidelity of $.73 \pm .02$ was achieved. The loss of signal is primarily due to spin relaxation, incomplete refocusing of couplings and intrinsic defects in using selective pulses. The success of the experiment derives from the use of the following techniques: 1. An RF imaging method to greatly reduce the effects of RF inhomogeneities. 2. A gradient based selection method for removing signal from the spin $\frac{3}{2}$ component of the methyl group in an almost optimal way. 3. The use of abstract reference frames for each nucleus to absorb chemical shift and first order off-resonance effects in selective pulses. 4. Precomputation of coupling effects during pulses. 5. A pulse sequence compiler that optimizes delays between pulses for achieving the desired amount of coupling evolution while minimizing unwanted couplings. All these techniques are scalable in principle. Further details are in the methods section.

The cat-state benchmark has three applications that promise to make it useful for NMR and other quantum technologies. First, the benchmark demonstrates the ability to reach the maximum coherence with little loss of signal. Previous experiments have generated coherences by exploiting symmetry and effective Hamiltonian methods. Very high order coherences can be observed in solid state [12]. A maximal coherence of order seven was detected by Weitekamp *et al.* [32] in benzene with one carbon labeled by exploiting symmetry. The methods used in these cases do not yield the amount of signal that can be achieved by using methods based on quantum networks.

Second, the output of the benchmark can be used as a very reliable pseudo-pure state for quantum algorithms. We can write the maximum coherence on n qubits as a sum of two operators $\tilde{X} = |00\dots\rangle\langle 11\dots| + |11\dots\rangle\langle 00\dots|$

and $\tilde{Y} = i|11\dots\rangle\langle 00\dots| - i|00\dots\rangle\langle 11\dots|$. The decoding operator converts \tilde{X} to $\sigma_x^{(1)}|0\dots\rangle\langle 0\dots|$ and \tilde{Y} to $\sigma_y^{(1)}|0\dots\rangle\langle 0\dots|$. These states can be used as a pseudo-pure input to a quantum algorithm using one less qubit, provided the following two problems are addressed: The first problem is to ensure that the labeling method can be used together with a subsequent algorithm. The second problem is to eliminate errors accumulated when decoding the n -coherence.

Clearly, the method used to label the n -coherence must be reliable. The gradient based method is effective in conjunction with a quantum algorithm, as long as the echo pulse is applied just before the final observation. Unfortunately, diffusion introduces loss of signal at the gradient strengths required when used with long algorithms. Also, gradient methods do not easily generalize to other proposed quantum devices—an important issue in benchmarking. To label the n -coherence one can instead perform $2n + 1$ experiments, where in the k 'th experiment, the gradient is replaced by explicit pulses that rotate each qubit by a phase $\phi_k = 2\pi k/(2n + 1)$. If o_k is the expectation of the observable measured at the end of the k 'th experiment, then the value $o = \sum_k o_k e^{-i2\pi kn/(2n+1)}$ is non-zero only for signal originating at the n -coherence. This technique can be applied in any system where it is possible to apply z -rotations reliably. If the phase of applied pulses is highly controllable (as is the case in systems controlled by RF or optical fields), instead of applying explicit pulses to accomplish the z -rotations, one can change the reference frame for each qubit, which is equivalent to changing the phase of all subsequent pulses and the observation reference phase by $-\phi_k$. This is essentially a phase cycling method for selecting the n -coherence [12]. We have used both the gradient based and this phase cycling method with identical results in the crotonic acid system.

The problem of decoding error can in principle be solved by using the maximum coherence directly as the input for a (modified) algorithm. However it is not possible to obtain a reference signal for the n -coherence without first mapping it to an accessible observable, which can involve a loss of signal. Another problem is that it may be inconvenient to use the n -coherence instead of the more familiar standard pseudo-pure state. Our experiments show that we can decode the n -coherence to the pseudo-pure state with no detectable error in the observed spectrum. There can be error signal in unobserved operators which one would like to eliminate from future observation. This can be done efficiently by performing multiple experiments, each with a random phase of 0deg or 180deg applied to qubits 2, 3, ..., a technique which is a special case of the randomized methods of [19]. The number of experiments that need to be performed depends on the desired level of suppression of possible error signals. N experiments result in suppression by a factor of $O(1/\sqrt{N})$.

The final application of the cat-state benchmark is as

an experiment to test the ability to coherently control a quantum system and demonstrate a fully coherent implementation of a non-trivial quantum algorithm. This is a critical issue for scalable quantum information processing, as scalable robustness requires that each operation has a maximum error below some threshold (which may depend on the types of errors) [1,18,20]. The known thresholds seem to be dauntingly small. Nevertheless, interesting small scale computations may be performable with much higher error per gate. Thus the ability to implement the cat-state benchmark with high fidelity is a good indication of what types of tasks can be accomplished in the system at hand. In addition, the decoding algorithm of the cat-state benchmark is an instance of the type of process required to perform fault-tolerant error-correction [28], which is believed to be a necessary subroutine in any large scale quantum computation. Our experiment involved a total of twelve useful two-qubit operations, so the fidelity of .73 suggests an error of about $.023 = .27/12$ per coupling gate. If this degree of control were available in the context of quantum communication, it would be close to the known thresholds [5].

The realization of the cat-state benchmark given here is in an ensemble setting. Most proposals for quantum devices involve individual systems with pure initial states. In these cases the benchmark can be modified by replacing the ensemble measurements by repetition to infer σ_k with sufficiently high signal to noise. The preparation step is replaced by a network that directly maps the available initial state to the cat state. Note that any evaluation of a quantum device involves substantial repetition, essentially replacing the ensemble measurement by an ensemble in time.

Methods. We used a Bruker DRX-500 NMR spectrometer with a triple resonance probe for our experiments. (The triple resonance probe is normally used for proton, carbon 13 and nitrogen 15; we used only the first two.) All the equipment used was standard with no specialized modifications. The chemical structure of trans-crotonic acid is given in Fig.2. Deuterated chloroform was used as the solvent. The chemical shifts (at 298K and 500Mhz) and coupling constants were experimentally determined to within .1Hz by direct analysis of the proton and carbon spectra (see Fig.2). This data was used to design selective pulse shapes and times. Only 90deg and 180deg rotations were used in the pulse sequence. The hard and selective pulses were analyzed by simulation on single and pairs of nuclei and represented optimally as a composition of phase shifts, $\sigma_z\sigma_z$ couplings and an ideal 90deg or 180deg pulse. The simulation is efficiently scalable, requiring $7(7+1)/2$ two qubit simulations for the seven qubit register. This permits elimination of most first order errors due to off-resonance and coupling effects without using specialized shapes. The computed phase shifts were absorbed into the rotating frame of each nucleus, while the computed coupling effects contributed to the coupling operations or were refocused. To implement quantum information processing tasks, we

began with an ideal quantum network expressed in terms of 90deg rotations and $1/(2J)$ coupling evolutions. Refocusing pulses are then inserted, and an optimizing pulse sequence compiler is used to determine the best choice of delays between pulses to achieve the desired evolution. The compiler permitted us to automate many of the tasks of translating a quantum network to a pulse sequence. Often smaller couplings cannot be perfectly refocused without an excessive number of pulses. Error due to imperfect refocusing is explicitly estimated by the compiler. The final pulse sequence used in our experiment required 48 pulses with an estimated signal loss due to coupling errors of .15.

To have accurate pulses, we have reduced the effect of RF inhomogeneities present in standard configurations by selecting signal based on RF power. The method first applies a 90deg excitation pulse to the methyl group followed by a sequence of pairs of 180deg rotations at phases of $\pm\phi_k$, where ϕ_k was determined from one of the selective pulse shapes we used (modified by an initial sequence to compensate for an off-resonance effect) and designed to cause a 90deg phase shift in the signal at an RF power of about $\pm 2\%$ of the ideal. At other powers, the effect is such that a phase cycle involving a change of sign of the 90deg phase shift eliminates the signal. A final pulse returns the selected signal along the z-axis in preparation for the next step. By calibrating the power, we were able to retain 25% of the signal compared to an unselected spectrum. This sequence also has the property of selecting signal from only the methyl group so that the initial state is $\sigma_z^{(M)}$.

The next step in the experiment required selecting the spin 1/2 component of the methyl group's state space. This can be accomplished by use of a three step sequence involving transfer of polarization to the adjacent carbon and terminated by a gradient "crusher" (Fig.3). The elimination of signal from the spin $\frac{3}{2}$ states was verified by three experiments involving observation of the signal on the adjacent carbon after transfer of the methyl polarization with different delays for coupling. One of the resulting spectra is shown in Fig.4 with the standard reference spectrum. We were unable to detect error signal above the noise.

The remaining steps of the experiments consist of the generation of the n -coherence, labeling the n -coherence, and the decoding operations to obtain the standard pseudo-pure state, which was observed on the methyl-carbon C_1 . We chose C_1 for making observations because all the couplings are adequately resolved there. The sequence is as described earlier, with judiciously inserted refocusing pulses and optimized delays. All the pulse phases were computed automatically for the nuclei's individual reference frames. Knowledge of the intended current state of a nucleus was exploited when that state is $|0\rangle\langle 0|$ or $|1\rangle\langle 1|$ to absorb the effects of couplings to that nucleus into the reference frame. The compiled pulse sequence, pulse shapes and other required information

needed for running on a Bruker spectrometer is available from the authors. Fig.5 shows the pseudo-pure state signal compared to a reference spectrum obtained after selection of the spin $\frac{1}{2}$ selection sequence on the methyl group. Errors can show up as peaks in positions different from the leftmost one. We could not detect such errors above the noise. The fidelity is given by the ratio of the intensity of the left most peak in the final signal to the intensity of a peak in the reference spectrum and was computed to be $.73 \pm .02$.

Acknowledgments. We thank C. Unkefer for help in synthesizing labeled crotonic acid, David Cory and Tim Havel for advice in using NMR spectrometers, S. Lacelle for suggesting the idea of using crotonic acid, D. Lemaster and G. Fernandez for daily help at the spectrometer and W.H. Zurek for encouraging us to exceed our expectations. This research was supported by the Department of Energy under contract W-7405-ENG-36 and the National Security Agency. We thank the Newton Institute, where part of this work was completed.

-
- [1] D. Aharonov and M. Ben-Or. Fault-tolerant quantum computation with constant error. In *Proceedings of the 29th Annual ACM Symposium on the Theory of Computing*, pages 176–188, New York, New York, 1996. ACM Press. quant-ph/9611025.
- [2] A. Barenco, C. H. Bennett, R. Cleve, D. P. DiVincenzo, N. Margolus, P. Shor, T. Sleator, J. Smolin, and H. Weinfurter. Elementary gates for quantum computation. *Phys. Rev. A*, 52:3457–3467, 1995.
- [3] C. Bennett, F. Bessette, G. Brassard, L. Salvail, and J. Smolin. Experimental quantum cryptography. *Journal of Cryptology*, 5:3–28, 1992.
- [4] M. F. Bocko, A. M. Herr, and M. J. Feldman. Prospects for quantum coherent computation using superconducting electronics. *IEEE Trans. App. Supercond.*, 7:3638–3641, 1997.
- [5] H.-J. Briegel, W. Dür, J. I. Cirac, and P. Zoller. Quantum repeaters for communication. quant-ph/9803056, 1998.
- [6] I. L. Chuang, N. Gershenfeld, and M. Kubinec. Experimental implementation of fast quantum searching. *Physical Review Letters*, 80:3408–3411, 1998.
- [7] I. L. Chuang, N. Gershenfeld, M. Kubinec, and D. Leung. Bulk quantum computation with nuclear magnetic resonance: Theory and experiments. *Proceedings of the Royal Society of London A*, 454:447–467, 1998.
- [8] I. L. Chuang, L. M. K. Vandersypen, X. Zhou, D. W. Leung, and S. Lloyd. Experimental realization of a quantum algorithm. *Nature*, 393:143–146, 1998. (Letter to Nature), quant-ph/9801037.
- [9] J. Cirac and P. Zoller. Quantum computations with cold trapped ions. *Physical Review Letters*, 74:4091–, 1995.
- [10] D. G. Cory, A. F. Fahmy, and T. F. Havel. Ensemble quantum computing by nmr-spectroscopy. *Proceedings of the National Academy of Sciences of the United States of America*, 94:1634–1639, 1997.
- [11] D. G. Cory, W. Maas, M. Price, E. Knill, R. Laflamme, W. H. Zurek, T. F. Havel, and S. S. Somaroo. Experimental quantum error correction. *Physical Review Letters*, 81:2152–2155, 1998. quant-ph/9802018, LA-UR-98-564.
- [12] L. Emsley and A. Pines. Lectures on pulsed nmr. In *Proceedings of the International School of Physics*, volume CXXIII, pages 2949–2954, 1994.
- [13] R. Freeman. *Spin choreography*. Oxford University Press, Oxford, UK, 1998.
- [14] N. A. Gershenfeld and I. L. Chuang. Bulk spin resonance quantum computation. *Science*, 275:350–356, 1997.
- [15] J. A. Jones and M. Mosca. Implementation of a quantum algorithm to solve deutsch’s problem on a nuclear magnetic resonance quantum computer. quant-ph/9801027, 1998.
- [16] J. A. Jones, M. Mosca, and R. H. Hansen. Implementation of a quantum search algorithm on a quantum computer. *Nature*, 392:344–346, 1998.
- [17] B. E. Kane. A silicon-based nuclear spin quantum computer. *Nature*, 393:133–137, 1998. (Article).
- [18] A. Yu. Kitaev. Quantum computations: algorithms and error correction. *Uspekhi Mat. Nauk*, 52:53–112, 1997.
- [19] E. Knill, I. Chuang, and R. Laflamme. Effective pure states for bulk quantum computation. *Phys. Rev. A*, 57:3348–3363, 1998. quant-ph/9706053.
- [20] E. Knill, R. Laflamme, and W. H. Zurek. Resilient quantum computation. *Science*, 279:342–345, 1998.
- [21] R. Laflamme, E. Knill, W. H. Zurek, P. Catasti, and S. V. S. Mariappan. Nmr-ghz. *Philosophical Transactions: Mathematical, Physical and Engineering Sciences A*, 356:1941–1948, 1997. quant-ph/9709025.
- [22] D. Loss and D. P. DiVincenzo. Quantum computation with quantum dots. cond-mat/9701055, 1997.
- [23] R. Marx, A. F. Fahmy, J. M. Myers, W. Bermel, and S. J. Glaser. Realization of a 5-bit nmr quantum computer using a new molecular architecture. quant-ph/9905087, 1999.
- [24] M. A. Nielsen, E. Knill, and R. Laflamme. Complete quantum teleportation. *Nature*, 396:52–55, 1998. LA-UR-98-4194.
- [25] V. Privman, I. D. Vagner, and G. Kventsel. Quantum computation in quantum-hall systems. quant-ph/9707017, 1997.
- [26] B. Schumacher. Sending entanglement through noisy quantum channels. *Phys. Rev. A*, 54:2614–2628, 1996. quant-ph/9604023.
- [27] A. Shnirman, G. Schön, and Ziv Hermon. Quantum manipulations of small josephson junctions. *Physical Review Letters*, 79:2371–2374, 1997.
- [28] P. W. Shor. Fault-tolerant quantum computation. In *Proceedings of the Symposium on the Foundations of Computer Science*, pages 56–65, Los Alamitos, California, 1996. IEEE press. quant-ph/9605011.
- [29] P. W. Shor. Polynomial-time algorithms for prime factorization and discrete logarithms on a quantum computer. *SIAM J. Comput.*, 26:1484–1509, 1997.
- [30] D. R. Simon. On the power of quantum computation. *SIAM J. Comput.*, 26:1474–1483, 1997.

- [31] O. W. Sørensen, G. W. Eich, M. H. Levitt, G. Bodenhausen, and R. R. Ernst. Product operator-formalism for the description of nmr pulse experiments. *Prog. Nuc. Mag. Res. Spect.*, 16, 1983.
- [32] D. P. Weitekamp, J. R. Garbow, and A. Pines. Determination of dipole coupling constants using heteronuclear multiple quantum nmr. *J. Chem. Phys.*, 77:2870–2883, 1982.
- [33] S. Wiesner. Conjugate coding. *Sigact News, (original manuscript ~1969)*, 15:78–88, 1983.

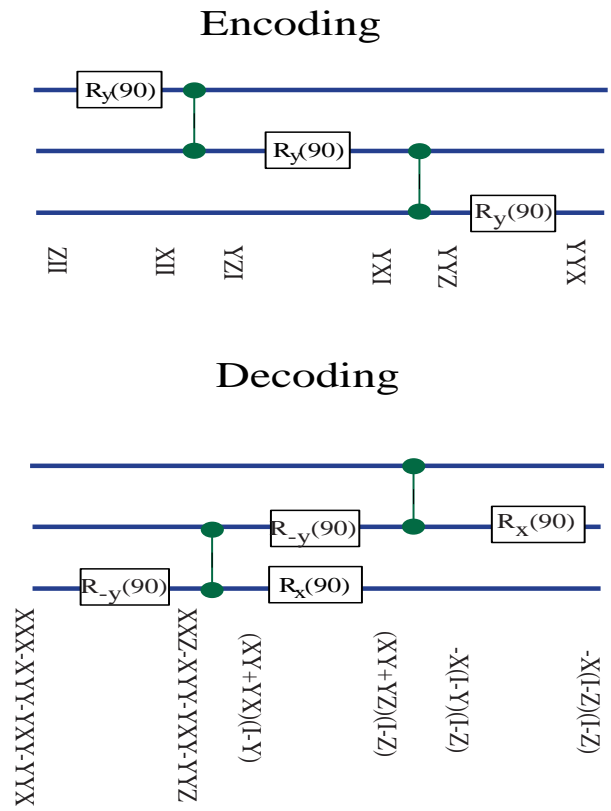


FIG. 1. Top: Encoding of the deviation matrix $\sigma_z II$ into $\sigma_y \sigma_y \sigma_x$ by using a cascade of rotations and J-couplings. A three coherence $|000\rangle\langle 111| + |111\rangle\langle 000|$ is contained in the output which can be labeled using a magnetic gradient or phase cycling. Bottom: Decoding the coherence to a pseudo-pure state is accomplished by a similar inverse cascade. The vertical text below the network denotes the state of the three qubits at that point in the network with $X = \sigma_x, Y = \sigma_y, Z = \sigma_z$. Both networks generalize by extending the cascade to more qubits.

	M	H ₁	H ₂	C ₁	C ₂	C ₃	C ₄
M	-969.4						
H ₁	6.9	-3560.3					
H ₂	-1.7	15.5	-2938.2				
C ₁	127.5	3.8	6.2	-2327.0			
C ₂	-7.1	156.0	-0.7	41.6	-18599.2		
C ₃	6.6	-1.8	162.9	1.6	69.7	-15412.8	
C ₄	-0.9	6.5	3.3	7.1	1.4	72.4	-21685.1

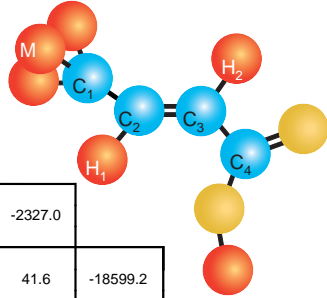


FIG. 2. Molecular structure of trans-crotonic acid together with a table of the chemical shifts and J -coupling constants. The chemical shifts are on the diagonal and are given with respect to reference frequencies of 500.13 MHz (protons) and 125.76 Mhz (carbons) on the 500 Mhz spectrometer we used. The T_2^* were greater than 2sec.

$M_{1/2}$ selection

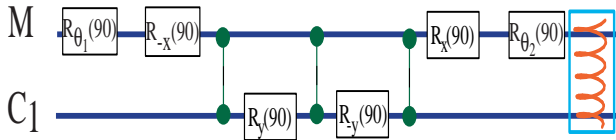


FIG. 3. Network to select the spin $\frac{1}{2}$ subspace of the methyl group. Refocusing needed to decouple the other nuclei are not shown. The spiral at the end is a gradient “crusher” to remove the transversal polarization.

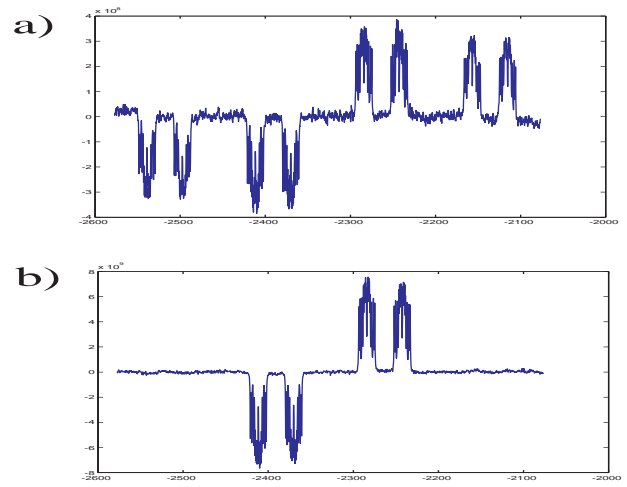


FIG. 4. Spectra of the methyl-carbon. Spectrum a) is obtained after transfer of the methyl equilibrium polarization to the carbon. Both the spin $\frac{1}{2}$ and the spin $\frac{3}{2}$ components are present. Only spin $\frac{3}{2}$ signal contributes to the extreme peak groups. Spectrum b) is obtained after transfer of the spin $\frac{1}{2}$ selected polarization from the methyl group. There is no signal in the extreme peak groups detectable above the noise. This together with two other, similar spectra (not shown) obtained after different delays for coupling demonstrates good selection of the spin $\frac{1}{2}$ component of the methyl group. The scales for the two spectra are different, the number of scans for a) and b) was 8 and 256 respectively.

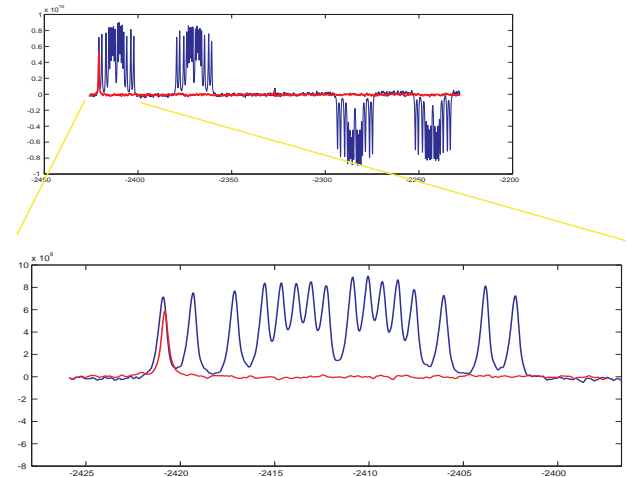


FIG. 5. Spectra of the pseudo-pure state (red) and the input state after transfer of polarization to the methyl-carbon (blue). Both spectra were acquired with 256 scans and are shown at the same scale. The signature of the pseudo-pure state is that only a single (the leftmost) peak remains. No detectable signal remains in any other peak position, the intensity ratio for the left most peak in the pseudo-pure state and the reference is $.73 \pm .02$.